Analysing powers and spin correlations in deuteron–proton charge exchange at 726 MeV

S. Dymov [a,b,*], T. Azaryan [b], Z. Bagdasarian [a,c], S. Barsov [d], J. Carbonell [e], D. Chiladze [c,a],
R. Engels [a], R. Gebel [a], K. Grigoryev [a,d], M. Hartmann [a], A. Kacharava [a], A. Khoukaz [f],
V. Komarov [b], P. Kulessa [g], A. Kulikov [b], V. Kurbatov [b], N. Lomidze [c], B. Lorentz [a],
G. Macharashvili [c,b], D. Mchedlishvili [c,a], S. Merzliakov [a,b], M. Mielke [f],
M. Mikirtychyants [a,d], S. Mikirtychyants [a,d], M. Nioradze [c], H. Ohm [a], D. Prasuhn [a],
F. Rathmann [a], V. Serdyuk [a], H. Seyfarth [a], V. Shmakova [b], H. Ströher [a], M. Tabidze [c],
S. Trusov [h,i], D. Tsirkov [b], Yu. Uzikov [b,j], Yu. Valdau [d,k], C. Weidemann [l], C. Wilkin [m]

[a] Institut für Kernphysik and Jülich Centre for Hadron Physics, Forschungszentrum Jülich, D-52425 Jülich, Germany
[b] Laboratory of Nuclear Problems, JINR, RU-141980 Dubna, Russia
[c] High Energy Physics Institute, Tbilisi State University, GE-0186 Tbilisi, Georgia
[d] High Energy Physics Department, Petersburg Nuclear Physics Institute, RU-188350 Gatchina, Russia
[e] Institut de Physique Nucléaire, Université Paris-Sud, IN2P3–CNRS, F-91406 Orsay Cedex, France
[f] Institut für Kernphysik, Universität Münster, D-48149 Münster, Germany
[g] H. Niewodniczański Institute of Nuclear Physics PAN, PL-31342 Kraków, Poland
[h] Institut für Kern- und Hadronenphysik, Forschungszentrum Rossendorf, D-01314 Dresden, Germany
[i] Skobeltsyn Institute of Nuclear Physics, Lomonosov Moscow State University, RU-119991 Moscow, Russia
[j] Department of Physics, M.V. Lomonosov Moscow State University, RU-119991 Moscow, Russia
[k] Helmholtz-Institut für Strahlen- und Kernphysik, Universität Bonn, D-53115 Bonn, Germany
[l] University of Ferrara and INFN, I-44100 Ferrara, Italy
[m] Physics and Astronomy Department, UCL, Gower Street, London, WC1E 6BT, UK

ARTICLE INFO

ABSTRACT

The charge exchange of vector polarised deuterons on a polarised hydrogen target has been studied in a high statistics experiment at the COSY-ANKE facility at a deuteron beam energy of $T_d = 726$ MeV. By selecting two fast protons at low relative energy E_{pp}, the measured analysing powers and spin correlations are sensitive to interference terms between specific neutron–proton charge-exchange amplitudes at a neutron kinetic energy of $T_n \approx \frac{1}{2} T_d = 363$ MeV. An impulse approximation calculation, which takes into account corrections due to the angular distribution in the diproton, describes reasonably the dependence of the data on both E_{pp} and the momentum transfer. This lends broad support to the current neutron–proton partial wave solution that was used in the estimation.

© 2015 The Authors. Published by Elsevier B.V. This is an open access article under the CC BY license (http://creativecommons.org/licenses/by/4.0/). Funded by SCOAP³.

It is a consequence of the nucleon spins that, assuming charge independence, five complex amplitudes are needed to describe neutron–proton elastic scattering [1]. This means that, above the pion production threshold, at least nine independent measurements are required at each scattering angle to allow an unambiguous partial wave decomposition. Some of the resulting observables, which could depend on up to three spin projections [2], are difficult to determine and values may only be obtained indirectly through combinations of other measurements.

It was shown several years ago [3] that, at small momentum transfers between the deuteron and the diproton, the tensor analysing power in the deuteron charge exchange on hydrogen, $\vec{d}p \to \{pp\}_s n$, is closely linked to the spin transfer in neutron–proton large angle scattering, $\vec{p}n \to \vec{n}p$, provided that the excitation energy E_{pp} in the final diproton is very low. Due to the Pauli principle the two protons are then dominantly in the $^1S_0$ state with antiparallel spins, here denoted by $\{pp\}_s$, so that there is then a spin–isospin flip to this state from the initial deuteron.

Further information on the neutron–proton scattering amplitudes can be obtained through measurements of the analysing powers and spin correlations in the $\vec{d}\vec{p} \to \{pp\}_s n$ reaction and measurements of this type were carried out at deuteron beam energies of $T_d = 1.2$ GeV and 2.27 GeV to investigate the np amplitudes at neutron kinetic energies of $T_n \approx \frac{1}{2}T_d = 600$ and 1135 MeV [4]. Both transverse spin correlations and the proton and deuteron analysing powers were investigated and the results were found to be consistent with modern partial wave solutions [5] at $T_n = 600$ MeV, while failing badly at 1135 MeV. We report here a similar investigation carried out at $T_d = 726$ MeV in a high statistics experiment, where tighter cuts could be placed on E_{pp} and small effects could be studied in detail. Since one might expect that the np partial wave amplitudes should be fairly reliable at 363 MeV, this is the ideal testing ground to establish quantitatively the validity of the theoretical modelling of deuteron charge exchange [6].

The experiment was undertaken using the ANKE magnetic spectrometer installed at an internal target position of the Cooler Synchrotron (COSY) at the Forschungszentrum Jülich [7]. Data were taken in parallel with those used to determine the spin correlations in quasi-free $\vec{n}\vec{p} \to \{pp\}_s \pi^-$ [8] and more details of the experimental procedure, in particular, of the measurements of the beam and target polarisations, are to be found in this reference.

Only deuteron beams with vector polarisation were used in this experiment and these had ideal values of $p_d^\uparrow = \frac{2}{3}$ and $p_d^\downarrow = -\frac{2}{3}$. The polarisations measured at the injection energy of 75.6 MeV with the low energy polarimeter were $p_d^\uparrow = +61 \pm 4\%$ and $p_d^\downarrow = -50 \pm 3\%$ for the two states, while the tensor polarisations were shown to be below 2%.

In order to increase the luminosity in the experiment, a jet of polarised atomic hydrogen was fed into a 25 μ thick teflon-coated aluminum storage cell target with dimensions $x \times y \times z = 15 \times 19 \times 390$ mm^3. Here the y-direction is perpendicular to the COSY plane and the x-direction is in this plane but perpendicular to the beam (z) direction. The polarisation, p_p, of the target was in the y-direction and its sign was reversed every five seconds. The mean value of the polarisation was determined through the study of the quasi-free $np \to d\pi^0$ asymmetry to be $|p_p| = 69\% \pm 2\%$(stat)$\pm 3.5\%$(syst). A more precise value of the product of the magnitudes of the beam and target polarisation was, however, extracted from an analysis of the pion production data themselves, which gave an average of $|p_d||p_p| = 0.373 \pm 0.015$ [8].[1]

Although the ANKE spectrometer is equipped with other elements, the only detector used in the charge-exchange experiment was the forward detector (FD) that identified and measured the two fast final protons from the $\vec{d}\vec{p} \to \{pp\}n$ reaction or, for polarisation studies, the fast deuteron and spectator proton from the $\vec{d}\vec{p} \to dp\pi^0$ reaction. The FD comprises a set of multiwire proportional and drift chambers and a two-plane scintillation hodoscope [9].

Having registered two charged particles in the FD, the isolation of the $dp \to ppn$ reaction depends on identifying these as protons on the basis of time-of-flight criteria that are described in detail in Ref. [4]. For this purpose the difference in the times of flight of the particles recorded in the FD is compared to that calculated on the assumption that the two particles are both protons. This procedure suppresses enormously the background that is associated, for example, with deuteron–proton pairs coming from dp elastic scattering.
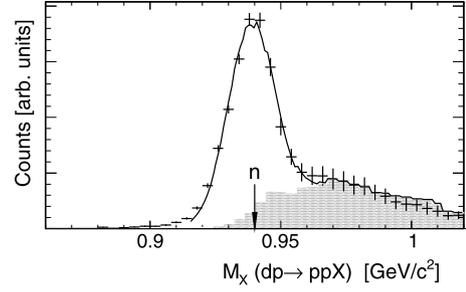

Fig. 1. Distribution in missing masses for the $dp \to ppX$ reaction for 726 MeV deuterons incident on a storage cell filled with polarised hydrogen. Events that originated from the walls of the cell gave rise to the tail at high M_X. The shape of this background was simulated by filling the cell with nitrogen gas and this led to the shaded area. The solid line represents the fit of a Gaussian plus the numerical values of the scaled background histogram.

The missing-mass M_X distribution of the identified $dp \to ppX$ reaction shows a striking peak around the mass of the missing neutron, as illustrated in Fig. 1. The long tail to higher missing masses arises from events originating from the walls of the storage cell. The shape of this background was simulated by filling the cell with nitrogen gas. This gave rise to the shaded area in the figure which, after normalising the distribution at high M_X, could be reliably subtracted bin by bin. The resulting $dp \to ppn$ events were then placed in 20 MeV/c bins in the momentum transfer q between the deuteron and diproton and 2 MeV bins in the diproton excitation energy E_{pp}.

For a vector polarised deuteron beam incident on a polarised hydrogen target, where both polarisations are in the y-direction, the ratio of the numbers of polarised $N(q, \phi)$ to unpolarised $N^0(q)$ events has the form [10]:

$$\frac{N(q,\phi)}{N^0(q)} = 1 + p_p A_y^p(q)\cos\phi + \frac{3}{2}p_d A_y^d(q)\cos\phi$$
$$+ \frac{3}{4}p_d p_p[(1 + \cos 2\phi)C_{y,y}(q) + (1 - \cos 2\phi)C_{x,x}(q)], \tag{1}$$

where the azimuthal angle ϕ is measured from the x-axis.

From studying the ϕ dependence of the count rates for the four combinations of beam and target polarisations it is possible to extract separately the values of the proton and deuteron vector analysing powers as well as the two spin correlations. The results for these observables are shown in Figs. 2 and 3. The deuteron vector analysing power A_y^d of Fig. 2 remains very small over our whole q range, only (possibly) exceeding 1% in magnitude for $q \gtrsim 120$ MeV/c. The proton analysing power A_y^p, though small, is much larger than A_y^d. These two features are very similar to the results found at 600 MeV per nucleon [4], though the statistical precision of the current data is much higher.

Due to the ANKE exit window being much wider in the horizontal direction than in the vertical, for the larger values of q the data are more populated near $\sin\phi = 0$. It follows from Eq. (1) that, in this limit, the spin correlation $C_{y,y}$ is better measured than $C_{x,x}$, and this is seen in Fig. 3. However, in order to assess the significance of these results we must turn to a reaction model.

In impulse approximation the amplitude for the $dp \to \{pp\}n$ charge-exchange reaction is proportional to the $np \to pn$ charge-exchange amplitude times a form factor that represents the overlap of the initial deuteron wave function with that of the outgoing diproton [3,6]. The elementary $np \to pn$ amplitude may be written in terms of five scalar amplitudes in the np c.m. frame as:

$$f_{np} = \alpha(q) + i\gamma(q)(\boldsymbol{\sigma}_1 + \boldsymbol{\sigma}_2) \cdot \boldsymbol{n} + \beta(q)(\boldsymbol{\sigma}_1 \cdot \boldsymbol{n})(\boldsymbol{\sigma}_2 \cdot \boldsymbol{n})$$
$$+ \delta(q)(\boldsymbol{\sigma}_1 \cdot \boldsymbol{m})(\boldsymbol{\sigma}_2 \cdot \boldsymbol{m}) + \varepsilon(q)(\boldsymbol{\sigma}_1 \cdot \boldsymbol{l})(\boldsymbol{\sigma}_2 \cdot \boldsymbol{l}), \tag{2}$$

---

[1] The dilution of the polarisation between the deuteron and the constituent neutron was minimised by preferentially selecting low Fermi momenta in the deuteron, as shown for the analogous case in Fig. 2a of Ref. [8].
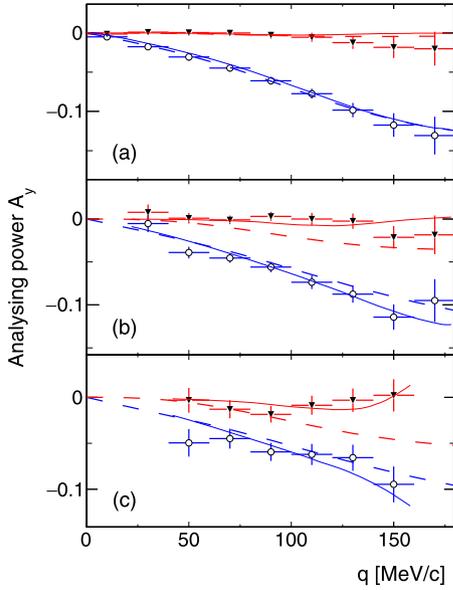
Fig. 2. Values of the deuteron (vector) analysing power A_y^d (black inverted triangles) and proton analysing power A_y^p (blue open circles) for the $dp \to \{pp\}n$ reaction at 726 MeV. Data were placed in bins of (a) $E_{pp} < 2$ MeV, (b) $4 < E_{pp} < 6$ MeV, and (c) $8 < E_{pp} < 10$ MeV; only statistical errors are shown. The curves are impulse approximation estimates [6] folded with experimental acceptance. These used the current SAID neutron–proton partial wave solution [5] as input. The dashed lines neglect the predicted dependence on the angle between the relative momentum in the diproton and the momentum transfer. The model predictions for this are included in the solid lines.
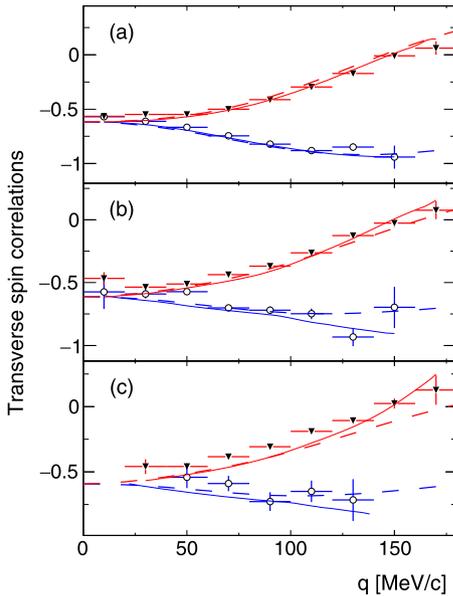
Fig. 3. Values of the spin correlations $C_{y,y}$ (black inverted triangles) and $C_{x,x}$ (blue open circles) for the $dp \to \{pp\}_s n$ reaction at 726 MeV. The conventions are identical to those of Fig. 2.

where $q = \sqrt{-t}$ is the three-momentum transfer between the initial neutron and final proton and the Pauli matrices $\boldsymbol{\sigma}$ are sandwiched between neutron and proton spinors. Of the unit basis vectors, $\boldsymbol{l}$ lies along the mean of the initial proton and final neutron momenta, $\boldsymbol{n}$ lies along $\boldsymbol{q}$, and $\boldsymbol{m} = \boldsymbol{n} \times \boldsymbol{l}$. It should be noted that the amplitudes of Eq. (2) are actually linear combinations of the standard elastic ones, defined for example in Ref. [2]. This important distinction arises because the spin dependence that is made explicit here is that corresponding to charge exchange [3,11].
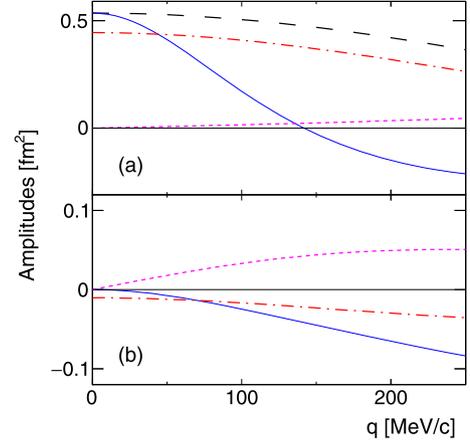
Fig. 4. Values of the (a) real and (b) imaginary parts of the np amplitudes at 363 MeV predicted on the basis of the current SAID PWA solution [5]. The amplitudes of Eq. (2), normalised to $d\sigma/dq^2$, have been rotated such that $\beta(q)$ is real. The curves are for β (black, long dashed), δ (blue, full), ϵ (red, dot-dashed), and γ (magenta, short dashed). It should be noted that the scales in panels (a) and (b) are very different.

Values of the amplitudes of Eq. (2) at 363 MeV can be extracted from the current partial wave solution of the SAID group [5] and the ones that are relevant to the current work are shown in Fig. 4 as functions of the momentum transfer q. Since only relative phases are significant in the discussion, these amplitudes have been rotated in the complex plane to make β real for all q. Apart from the obvious features that $\beta = \delta$ and $\gamma = 0$ at $q = 0$, the most notable behaviour is the zero in the δ amplitude at $q \approx (140 - 10i)$ MeV/c. This amplitude is strongly influenced by one pion exchange and, in the simplest distorted model, this has a zero when $q = m_\pi c$, where m_π is the mass of the charged pion.

Although the resulting $dp \to \{pp\}n$ amplitudes will be evaluated taking into account higher partial waves in the pp system, using an update of the program of Ref. [6], it is useful for a qualitative discussion to consider the results that follow if one retains only the pp $^1S_0$ configuration that dominates at low E_{pp}. In this case the impulse approximation model predicts that:

$$A_y^d = 0,$$
$$A_y^p = -2\,Im(\beta^*\gamma)/(|\beta|^2 + |\gamma|^2 + |\varepsilon|^2 + |\delta|^2),$$
$$C_{y,y} = -2\,Re(\varepsilon^*\delta)/(|\beta|^2 + |\gamma|^2 + |\varepsilon|^2 + |\delta|^2),$$
$$C_{x,x} = -2\,Re(\varepsilon^*\beta)/(|\beta|^2 + |\gamma|^2 + |\varepsilon|^2 + |\delta|^2). \tag{3}$$

In addition to taking the higher pp partial waves into account, away from $q = 0$ these formulae have to be modified to include the effects of the deuteron D-wave and the Wigner rotation that arises from a change in reference frame [3].

In the $^1S_0$ limit of the impulse approximation the spin correlations are linked at $q = 0$ to a combination of neutron–proton spin-correlation and spin-transfer parameters, as defined in Ref. [2], through

$$C_{x,x}(0) = C_{y,y}(0) = \frac{2[A_{00nn}(\pi) - D_{n0n0}(\pi)]}{3 - K_{0ll0}(\pi) - 2K_{0nn0}(\pi)}. \tag{4}$$

The curves shown in Fig. 2a and Fig. 3a represent the full impulse approximation calculations for $E_{pp} < 2$ MeV [6]. Though in this case the two protons should be dominantly in the $^1S_0$ configuration, there might still be some small deviation from the $A_y^d = 0$ prediction of Eq. (3). However, both the data and the predictions are at the 1% level and it is hard to draw firm conclusions in view

of the systematic uncertainties. The situation is much clearer for the proton analysing power of Fig. 2a, where the current SAID solution provides a quantitative description of the experimental data. Since the real and imaginary parts of γ in Fig. 4 are of comparable size, this suggests that the phase between β and γ is well reproduced in the partial wave solution [5].

The general shapes of the $C_{x,x}$ and $C_{y,y}$ predictions in Fig. 3a are very much in line with the measured data though there are some quantitative differences. $C_{y,y}$ changes sign, as one would expect from the simple one-pion-exchange contribution to the δ amplitude, though this happens at a few MeV/c higher than the prediction. While being independent of the uncertainties in the beam and target polarisations, this crossing is a very sensitive test of the δ/ϵ interference because of the presence of the small imaginary part in the zero of the δ amplitude at $q \approx (140 - 10i)$ MeV/c.

The prediction of $C_{x,x}(0) \approx -0.62$ at $q = 0$ is to be compared to the value of ≈ -0.57 extracted from the experimental data for $E_{pp} < 2$ MeV. The significance of the discrepancy here must be judged against the systematic uncertainties in the experiment and the modelling. Systematic effects in the data could arise, for example, from the choice in fitting limits combined with some imperfection in the background description, but these can be estimated conservatively to be below 0.01 for the analysing powers and 0.03 for the spin correlations. To these must be added the 4% associated with the product of the beam and target polarisations. The uncertainties arising from the beam or target polarisations are small compared to the statistical errors in A_y^d and A_y^p.

The SAID single-energy solution yields error bars on the np spin-transfer and correlation parameters needed to evaluate Eq. (4). The resulting uncertainty in $C_{x,x}(0)$ of ± 0.024 [12] is very much a lower limit because it does not include any uncertainties in the model assumed in the SAID analysis or in the data selection [5]. It must also be stressed that few of the four np observables appearing in Eq. (4) have been directly measured near 180°. Furthermore, the SAID predictions do show very strong angular dependence, which makes any extrapolation in angle less reliable. On the other hand, the uncertainty of 4% in the product of the beam and target polarisations would correspond to a systematic error of ± 0.025 in the determination of $C_{x,x}(0)$.

The $\vec{d}\vec{p} \to \{pp\}_s n$ data were here described using a plane wave impulse approximation [3,6] and the largest correction to this picture is likely to come from double scattering inside the deuteron. Evaluating the $^1S_0$ contribution in an eikonal approach, it has been shown that the spin dependence of the deuteron tensor analysing powers is little changed by this correction for $q \lesssim 140$ MeV/c [13]. An estimation of the double scattering [3,13] at $q = 0$ indicates that this modifies the prediction for $C_{x,x}(0)$ by only 0.003. This is an order of magnitude less than the quoted uncertainties and so can be safely neglected.

For larger values of E_{pp}, P and higher waves become significant so that the angular distribution in the diproton is no longer isotropic. If $\boldsymbol{k}$ is the relative momentum in the diproton, then $E_{pp} = k^2/m$, where m is the proton mass. At large values of k and q, where the effects of the Pauli exclusion principle and final state interactions are small, there will be a quasi-free peak at $\boldsymbol{k} = \pm \boldsymbol{q}/2$. Quite generally therefore, away from the small E_{pp} region

there will be a significant dependence on the angle θ_{kq} between $\boldsymbol{k}$ and $\boldsymbol{q}$ [3]. It is important to note that this effect is already included in the computer program of Ref. [6].

Panels b and c of Figs. 2 and 3 show the experimental results obtained in the bins $4 < E_{pp} < 6$ MeV indicate the plane wave impulse approximation prediction where one ignores the angular distribution in θ_{kq}. When the predictions [6] of this angular dependence are included one obtains the solid lines in the figures. Though most of the changes are small compared to the uncertainties in the np input data, these generally go in the right direction, especially for the deuteron vector analysing power. The same is also true for the results in two E_{pp} bins that are not shown here.

Spin correlations and analysing powers have been measured in deuteron charge exchange on hydrogen, $\vec{d}\vec{p} \to \{pp\}n$, at a beam energy of 726 MeV. The high statistics of this experiment allowed tight cuts to be placed on the pp excitation energy E_{pp}. The agreement of these data with the impulse approximation model at very low E_{pp}, where the $^1S_0$ state will be dominant, shows that the np amplitudes obtained from partial wave analysis [5] must be broadly correct. There are slight discrepancies near the forward direction but these are of such a size that they could originate from the partial wave solution or from uncertainties in the experimental data presented here.

At larger values of E_{pp} there are small effects associated with P and higher partial waves in the pp system that lead to some non-isotropy in the diproton angular distribution. These were studied by putting the data in five 2 MeV bins in E_{pp}. Though the acceptance in ANKE is less complete at large vales of E_{pp}, the plane wave impulse approximation model describes all these effects.

Acknowledgements

References

[1] M.H. McGregor, M.J. Moravcsik, H.P. Stapp, Annu. Rev. Nucl. Sci. 10 (1960) 291.
[2] J. Bystricky, F. Lehar, P. Winternitz, J. Phys. (Paris) 39 (1978) 1.
[3] D.V. Bugg, C. Wilkin, Nucl. Phys. A 467 (1987) 575.
[4] D. Mchedlishvili, et al., Eur. Phys. J. A 49 (2013) 49.
[5] R.A. Arndt, I.I. Strakovsky, R.L. Workman, Phys. Rev. C 62 (2000) 034005;
    R.A. Arndt, W.J. Briscoe, I.I. Strakovsky, R.L. Workman, Phys. Rev. C 76 (2007) 025209;
    http://gwdac.phys.gwu.edu.
[6] J. Carbonell, M.B. Barbaro, C. Wilkin, Nucl. Phys. A 529 (1991) 653.
[7] S. Barsov, et al., Nucl. Instrum. Methods A 462 (1997) 364.
[8] S. Dymov, et al., Phys. Rev. C 88 (2013) 014001.
[9] S. Dymov, et al., Part. Nucl. Lett. 2 (119) (2004) 40.
[10] G.G. Ohlsen, Rep. Prog. Phys. 35 (1972) 717.
[11] F. Lehar, C. Wilkin, Phys. Part. Nucl. Lett. 7 (2010) 235.
[12] R. Workman, private communication, 2014.
[13] C. Wilkin, in: L. Blokhintsev, I.I. Strakovsky (Eds.), NN and 3N Interactions, Nova Science, N.Y., 2014.